

THE DIURNAL VARIATION OF THE NEUTRAL SODIUM SPECIES IN  
THE UPPER ATMOSPHE. (U) ATMOSPHERIC AND ENVIRONMENTAL  
RESEARCH INC CAMBRIDGE MA J M RODRIGUEZ ET AL.

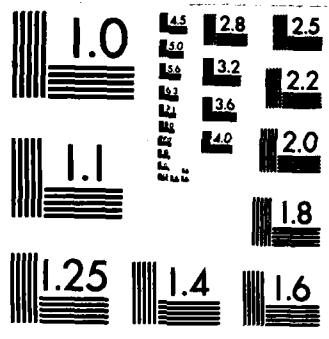
UNCLASSIFIED

01 AUG 84 AFGL-TR-84-0204 F19628-83-C-0123 F/G 4/1

NL

END

4110



MICROCOPY RESOLUTION TEST CHART  
NATIONAL BUREAU OF STANDARDS-1963-A



AFGL-TR-84-0204

AD-A154 988

THE DIURNAL VARIATION OF THE NEUTRAL SODIUM  
SPECIES IN THE UPPER ATMOSPHERE:  
A MODEL STUDY

José M. Rodriguez  
Malcolm K. W. Ko  
Nien Dak Sze

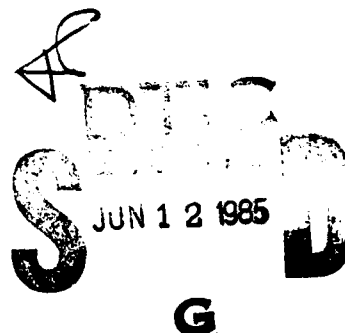
Atmospheric and Environmental Research, Inc.  
840 Memorial Drive  
Cambridge, Massachusetts 02139

Scientific Report No. 1

1 August 1984

Approved for public release; distribution unlimited

AIR FORCE GEOPHYSICS LABORATORY  
AIR FORCE SYSTEMS COMMAND  
UNITED STATES AIR FORCE  
HANSCOM AFB, MASSACHUSETTS 01731



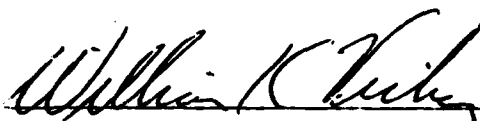
85 5 17 03 8

DTIC FILE COPY

This technical report has been reviewed and is approved for publication.

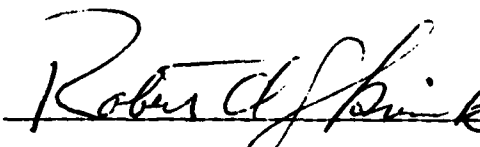


WILLIAM SWIDER  
Contract Manager



WILLIAM K. VICKERY, Acting Chief  
Ionospheric Disturbances & Modification Branch

FOR THE COMMANDER



ROBERT A. SKRIVANEK, Director  
Ionospheric Physics Division

This report has been reviewed by the ESD Public Affairs Office (PA) and is releasable to the National Technical Information Service (NTIS).

Qualified requestors may obtain additional copies from the Defense Technical Information Center. All others should apply to the National Technical Information Service.

If your address has changed, or if you wish to be removed from the mailing list, or if the addressee is no longer employed by your organization, please notify AFGL/DAA, Hanscom AFB, MA 01731. This will assist us in maintaining a current mailing list.

Unclassified

SECURITY CLASSIFICATION OF THIS PAGE

ADA154 988

## REPORT DOCUMENTATION PAGE

1a. REPORT SECURITY CLASSIFICATION Unclassified		1b. RESTRICTIVE MARKINGS	
2a. SECURITY CLASSIFICATION AUTHORITY		3. DISTRIBUTION/AVAILABILITY OF REPORT Approved for public release; distribution unlimited	
2b. DECLASSIFICATION/DOWNGRADING SCHEDULE		4. PERFORMING ORGANIZATION REPORT NUMBER(S)	
5. MONITORING ORGANIZATION REPORT NUMBER(S) AFGL-TR-84-0204		6a. NAME OF PERFORMING ORGANIZATION Atmospheric and Environmental Research Inc.	
6b. OFFICE SYMBOL (If applicable)		7a. NAME OF MONITORING ORGANIZATION	
6c. ADDRESS (City, State and ZIP Code) 840 Memorial Drive Cambridge, MA 02139		7b. ADDRESS (City, State and ZIP Code)	
8a. NAME OF FUNDING/SPONSORING ORGANIZATION Air Force Geophysics Laboratory		8b. OFFICE SYMBOL (If applicable)	
9. PROCUREMENT INSTRUMENT IDENTIFICATION NUMBER F19628-83-C-0123		10. SOURCE OF FUNDING NOS.	
11. TITLE (Include Security Classification) The Diurnal Variation of the Neutral Sodium Species in the Upper Atmosphere: A Model Study Rodriguez, José M., Ko K.W., Malcolm, and Sze Nien Dak		PROGRAM ELEMENT NO. 61102F	
12. PERSONAL AUTHOR(S)		PROJECT NO. 2310	
13a. TYPE OF REPORT Sci Rpt No. 1		TASK NO. G3	
13b. TIME COVERED FROM _____ TO _____		WORK UNIT NO. BA	
14. DATE OF REPORT (Yr., Mo., Day) 1984 August 1		15. PAGE COUNT 29	
16. SUPPLEMENTARY NOTATION			
17. COSATI CODES		18. SUBJECT TERMS (Continue on reverse if necessary and identify by block number)	
FIELD	GROUP	SUB. GR.	
		Sodium, Upper Atmosphere, Mesosphere Photochemistry	
19. ABSTRACT (Continue on reverse if necessary and identify by block number) -A study is made to calculate the diurnal behavior of the neutral sodium species (Na, NaO, NaO <sub>2</sub> , and NaOH) in the mesosphere using a one-dimensional photochemical model. The calculated results for Na are compared with available observations. The model results show that NaO <sub>2</sub> is an important reservoir for the sodium species in the atmosphere, and that the diurnal variation of Na in the mesosphere is, to a large extent, determined by the diurnal behavior of atomic oxygen. The role of NaOH as a temporary reservoir for sodium and its possible effect on stratospheric chlorine chemistry remains unclear, as there is insufficient information from observation of Na to determine the rate for the atmospheric production of NaOH.			
20. DISTRIBUTION/AVAILABILITY OF ABSTRACT UNCLASSIFIED/UNLIMITED <input type="checkbox"/> SAME AS RPT. <input checked="" type="checkbox"/> DTIC USERS <input type="checkbox"/>		21. ABSTRACT SECURITY CLASSIFICATION Unclassified	
22a. NAME OF RESPONSIBLE INDIVIDUAL William Swider		22b. TELEPHONE NUMBER (Include Area Code) (617)861-2109	
		22c. OFFICE SYMBOL LID	

# ABSTRACT

A study is made to calculate the diurnal behavior of the neutral sodium species (Na, NaO, NaO<sub>2</sub>, and NaOH) in the mesosphere using a one-dimensional photochemical model. The calculated results for Na are compared with available observations. The model results show that NaO<sub>2</sub> is an important reservoir for the sodium species in the atmosphere, and that the diurnal variation of Na in the mesosphere is, to a large extent, determined by the diurnal behavior of atomic oxygen. The role of NaOH as a temporary reservoir for sodium and its possible effect on stratospheric chlorine chemistry remains unclear, as there is insufficient information from observation of Na to determine the rate for the atmospheric production of NaOH.

Accession For	
NTIS GRA&I	<input checked="" type="checkbox"/>
DTIC TAB	<input type="checkbox"/>
Unannounced	<input type="checkbox"/>
Justification	
By	
Distribution/	
Availability Codes	
Dist.	Avail and/or Special
A/1	



## 1. INTRODUCTION

The existence of trace amounts of atomic sodium (Na) in the Earth's upper atmosphere was deduced in the earlier part of this century from observations of nighttime airglow in the D lines of Na (Chapman, 1939, and references there given). Subsequent measurements of resonance radiation in the D lines were carried out at twilight and during the day by numerous investigators in the period prior to 1970 (see review by Kvifte, 1973). These measurements deduced the concentration of atomic sodium in a narrow layer centered at around 90 km. The advent of laser radar techniques (lidar) has produced a wealth of information on the altitude distribution and the diurnal and seasonal variation of the sodium layer during the past 15 years (Gibson and Sandford, 1971, 1972; Megie and Blamont, 1977; Simonich et al., 1979; Clemesha et al., 1982; Granier and Megie, 1982). Although different mechanisms were originally proposed to explain the origin of this sodium layer (Kvifte, 1973), experimental evidence and present theoretical models favor a source from ablation of meteorites occurring between 80 and 100 km (Megie and Blamont, 1977; Gadsden, 1968; Hunten et al., 1980).

The first photochemical model for sodium compounds was proposed in 1939 by Chapman to explain the nighttime D-line emission. This mechanism proceeds through the oxidation-reduction cycle involving Na and sodium monoxide (NaO)



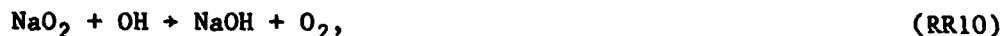
where the dissociation energy of  $\text{O}_2$  is partially channelled into the excitation of Na to the  $^2\text{P}$  state, with subsequent radiation in the D lines. The validity of the above mechanism has been confirmed by kinetic studies and atmospheric observations during the past 40 years. The evidence against the possibility of other mechanisms has been recently summarized by Bates and Ojha (1980).

The existence and chemistry of sodium compounds other than atomic sodium is more uncertain, because of a lack of laboratory kinetic data and atmospheric

---

\*RR numbers refer to reaction numbers in Table 1.

measurements. The non proton-hydrate positive ions observed in the middle atmosphere by Arnold et al. (1978) were originally interpreted to be of the form  $\text{NaOH}_2^+(\text{NaOH})_m(\text{H}_2\text{O})_n$  (Ferguson, 1978). This interpretation led Liu and Reid (1979) to postulate the production of NaOH through reactions such as



where  $\text{NaO}_2$  is produced by the reaction



This model predicted rapid conversion of Na to NaOH below an altitude of 90 km. Direct production of NaOH from NaO was proposed by Murad and Swider (1979) through the reaction



Although more recent measurements of stratospheric positive ions have eliminated the possibility of a sodium core (Arnold et al., 1981), the NaOH sources represented by reactions (RR10,RR11) and (RR7) still remain a possibility.

The abundance of NaOH is also of interest for stratospheric ozone chemistry. Murad and Swider (1979) and Murad, Swider, and Benson (1981) pointed out that the reaction



could constitute an important reaction pathway for stratospheric HCl if its rate were of the order of  $10^{-12} \text{ cm}^3 \text{ s}^{-1}$ , and if the NaOH concentration were  $\sim 10^5 \text{ cm}^{-3}$ . Furthermore, if NaCl were sufficiently stable to act as a nucleating agent and be incorporated into aerosols, reaction (1) could provide an important sink for stratospheric chlorine. The value of the rate for reaction (1) has recently been measured to be  $2.5 \times 10^{-10} \text{ cm}^3 \text{ s}^{-1}$  (Silver, Stanton,



Zahniser, and Kolb, 1984a). However, Rowland and Rogers (1982) indicated that photolysis of NaCl



could have a value of  $\sim 10^{-2} \text{ s}^{-1}$  if the observed UV absorption cross section of NaCl is taken to be its photodissociation cross section. In this case, the sequence of reactions (1) and (2) acts as a catalytic cycle converting the relatively stable HCl into active Cl. Determination of the importance of reactions (1) and (2) in the stratosphere awaits the measurement of unknown kinetic rates, in particular the production of NaOH (RR7).

More recently, the rate for RR3 has been measured (Husain and Plane, 1982; Silver, Zahniser, Stanton, and Kolb, 1984b) to have a value three orders of magnitude higher than that used in Liu and Reid's model. Such high values for the rate of RR3 raised the possibility of the existence of large amounts of NaO<sub>2</sub> in the upper atmosphere, with consequently low concentrations of atomic sodium. Analysis of the latest thermochemical data led Sze, Ko, Murad, and Swider (1982) to propose the reaction



as a potentially-fast recycling mechanism for NaO<sub>2</sub>.

Our present understanding of the chemistry of sodium compounds is summarized in Figure 1, based on the scheme of Sze, Ko, Murad, and Swider (1982). Because of the difficulty in manipulating gas-phase Na in the laboratory, kinetic data for reactions involving sodium are almost nonexistent. Besides the measurement of the rate for RR3, experimental data exists only for the photolysis of NaOH (RR4) (Rowland and Makide, 1982). However, constraints can be placed on the rate for RR1 and RR2 from the observed D-line emission, the measured background concentrations of O and O<sub>3</sub>, and kinetic considerations (Bates and Ojha, 1980). Additional constraints on other reaction rates can be obtained by comparing calculations with observations of the distribution (Liu and Reid, 1979; Sze, Ko, Murad, and Swider, 1982; Thomas, Isherwood, and Bowman, 1983) and diurnal variation of sodium (Kirchoff and Clemesha, 1983; Kirchoff, 1983). Estimated rates are given in Table 1 where laboratory measurements do not exist.

In Figure 1, the Na-NaO on the left-hand side represents the original Chapman scheme. The rates for RR1 and RR2 are sufficiently fast that the  $[Na]/[NaO]$  should be proportional to the  $[O]/[O_3]$  at any time of the day. Thus, in the absence of other sodium species, the diurnal behavior of the Na and NaO would be determined entirely by the diurnal variations of O and  $O_3$ . The species  $NaO_2$  and NaOH act as temporary reservoirs for the sodium species during the diurnal cycle. With the short photolysis lifetime for NaOH, diurnal variation of Na is expected if the density of NaOH is sufficiently high. The effect of  $NaO_2$  on the diurnal variation of Na would depend on the magnitude of the recycling reactions (RR5 and RR6).

We present in this report the results of our calculations of the diurnal variation of sodium compounds. Comparison of our results with the observed properties that are determined by photochemical processes can place additional constraints on some of the reaction rates. In particular, we will see that although RR6 must be slow, a fast rate for RR7 is consistent with present observations. Our study will also isolate the chemical cycles controlling the distribution and diurnal behavior of the sodium layer, thus estimating the sensitivity of our results to unknown kinetic rates and properties of the background atmosphere.

Section 2 summarizes the experimental information about atmospheric sodium available at present. Our model is described in Section 3, and the results of our calculations are presented in Section 4. Conclusions of our study are discussed in Section 5.

## 2. SUMMARY OF EXPERIMENTAL DATA

An extensive data base now exists providing detailed information on the diurnal and seasonal behavior of the sodium layer. Some of these properties are directly attributable to transport phenomena on a seasonal (Gibson and Sandford, 1971; Megie et al., 1978; Kirchoff et al., 1981; Kirchoff and Clemesha, 1983) or diurnal time scale (Megie and Blamont, 1977; Clemesha et al., 1978; Kirchoff et al., 1981; Clemesha et al., 1982). Nevertheless, we can deduce from the data certain characteristics that have direct relevance to photochemical processes. The experimental data to be used in constraining our model are as follows:

- a) Total Abundance of Atomic Sodium: Lidar observations have constrained the diurnal variation of the Na column density to less than 15% (Gibson and Sandford, 1972; Clemesha et al., 1982). The absolute magnitude of the total abundance ranges from a summer minimum of  $\sim 2 \times 10^9 \text{ cm}^{-2}$  to a winter maximum of  $6-8 \times 10^9 \text{ cm}^{-2}$ , yielding an average column density of  $4 \times 10^9 \text{ cm}^{-2}$ .
- b) Altitude Profiles of Atomic Sodium: Lidar observations of the sodium layer at different latitudes have consistently deduced a peak density of  $3-5 \times 10^3 \text{ cm}^{-3}$  at 90-92 km during periods of low meteoritic activity (Megie and Blamont, 1977; Simonich et al., 1979). The peak height and density correlates with the seasonal change in total abundance, with high column densities corresponding to low peak altitudes and high peak densities (Gibson and Sandford, 1971). Diurnal variations in the peak height have also been observed, but they are probably due to transport effects of gravity waves (Clemesha et al., 1982).
- c) Diurnal Variation of Local Densities of Atomic Sodium: The densities measured by lidar techniques exhibit a diurnal variation below 84 km (Simonich et al., 1979; Clemesha et al., 1982). The nocturnal decrease in sodium densities observed by these authors is about a factor of 2 at 83 km and 10 at 81 km.
- d) D-line Emission Rates: Measurements of the nighttime D-line emission in the southern hemisphere (low latitude) yield minimum values of 30 Rayleigh (R) during winter and 60 to 100 R at equinox (Kirchoff et al., 1981). Mean intensities in the northern hemisphere range from 35 to 100 R (Fukuyama, 1977). The seasonal variation in the northern hemisphere measurements is most pronounced at low latitudes, with amplitudes in agreement with the southern hemisphere results. The emission rate also exhibits a small nocturnal variation of 30% symmetric around a minimum at midnight (Kirchoff et al., 1981).

A summary of the above experimental constraints is given in Table 2. We will concentrate on the diurnal variation of the above quantities. However, the seasonal behavior will be useful for placing bounds on the experimental values used in comparison to our one-dimensional model.

### 3. DESCRIPTION OF MODEL

The one-dimensional model of mesospheric trace gases covers the altitude range from 60-100 km. It is an extension of the model previously used in studies of stratospheric chemistry (Sze, Ko, Specht, and Livshits, 1980). Concentrations of short-lived photochemical species are calculated using the grouping technique previously employed in stratospheric models (Sze et al., 1980).

The species calculated in our model include:

oxygen species,  $O_x$ :  $O(^1D)$ ,  $O$ ,  $O_3$

odd hydrogen species,  $HO_x$ :  $H$ ,  $OH$ ,  $HO_2$ ,  $H_2O_2$

odd nitrogen species,  $NO_x$ :  $N$ ,  $NO$ ,  $NO_2$ ,  $HNO_3$ ,  $NO_3$ ,  $N_2O_5$ ,  $HO_2NO_2$

sodium species,  $NaX$ :  $Na$ ,  $NaO$ ,  $NaO_2$ ,  $NaOH$

In addition,  $O_2(^1\Delta_g)$  is also included. Although the  $NO_x$  species and  $O_2(^1\Delta_g)$  are of minor importance in the neutral chemistry of the odd-oxygen and odd-hydrogen species, they are included in the chemistry scheme in anticipation of their roles in the ion chemistry. The effect of the odd-chlorine and methyl families on the above species is negligible at these altitudes; thus, they have not been included in the model.

Background species which are held fixed in the model include  $H_2$ ,  $H_2O$ ,  $CO$ ,  $N_2O$ ,  $O_2$ , and  $N_2$ . Densities of the major constituents ( $N_2$  and  $O_2$ ) and temperatures are taken from the U.S. Standard Atmosphere (1976). The densities of the background trace species  $CO$ ,  $H_2$ , and  $H_2O$ , are taken from Allen, Lunine, and Yung (1984).

Photochemical lifetimes for  $HO_x$  and  $O_x$  are shorter than one day at altitudes below 80 km. The concentrations of all constituents are calculated from the time-dependent equation

$$\frac{dn_i}{dt} = P_i - L_i n_i, \quad (3)$$

where  $n_i$ ,  $P_i$ , and  $L_i$  denote the density, production, and loss frequency for the  $i^{th}$  species. Equation (3) is solved subject to periodic boundary conditions over a 24-hour period,

$$n_i(t + 24 \text{ hrs.}) = n_i(t). \quad (4)$$

Note that the effect of transport is ignored in this region.

Time constants for  $\text{HO}_x$ ,  $\text{O}_x$ , and  $\text{NO}_x$  become much longer than one day above 90 km. The densities of the above constituents are then determined by down-gradient diffusion. Although it is within the capability of the model to calculate the distribution of the long-lived species, we have fixed their densities in our calculations to the profiles given by Allen et al., (1984) for  $\text{HO}_x$  and  $\text{O}_x$ , and by Solomon, Crutzen, and Roble (1982) for  $\text{NO}_x$ .

Sharp vertical gradients in the densities of  $\text{O}_x$  and  $\text{HO}_x$  result in very short ( $\sim 1$  day) transport time constants between 80 and 85 km. The diurnal variation of the above species is then determined by both photochemical and transport processes. The effects of transport are approximately accounted for in the present calculation by introducing an extra time-independent term,  $P_1^*$  in equation (3). The magnitude and sign of  $P_1^*$  is chosen such that the solutions of equation (3) at noon agree with the values calculated by Allen et al., (1984) at the same time.

The total density of sodium species ( $\text{NaX}$ ) is calculated assuming an incoming flux of  $2 \times 10^4 \text{ cm}^{-2} \text{ s}^{-1}$  at 100 km. The sodium is transported by diffusion into the troposphere where it is removed by heterogeneous processes with an effective lifetime of 10 days. The values of the diffusion coefficients below 70 km are the same as those used in the stratospheric model (Sze, Ko, Specht, and Livshits, 1980). Above 70 km, a value of  $10^6 \text{ cm}^2 \text{ s}^{-1}$  is adopted as suggested by Hunten (1975). The calculated total  $\text{NaX}$  volume mixing ratio ranges from  $2.3 \times 10^{-9}$  at 100 km to  $1 \times 10^{-11}$  at 60 km.

The chemical scheme for the oxygen, hydrogen, and nitrogen species is similar to the one used in the stratospheric model. Reaction rates are taken from the latest NASA review (JPL, 1982), with the corrections suggested by Allen et al., (1984). The reactions involving sodium species are taken from Sze, Ko, Murad, and Swider (1982) as given in Table 1.

#### 4. RESULTS

Diurnal profiles for the main  $\text{O}_x$  species ( $\text{O}$ ,  $\text{O}_3$ ) at 82, 84, 86, and 88 km are shown in Figures 2a, 2b, 2c, and 2d, respectively; similar profiles at the same altitudes are shown for the  $\text{HO}_x$  species,  $\text{H}$ ,  $\text{OH}$ , and  $\text{HO}_2$  in Figures 3a, 3b, 3c, and 3d. The calculations are performed for  $38^\circ\text{N}$ , summer solstice conditions. Our results are similar to the diurnal variation calculated by Allen

et al., (1984). The  $O_x$  and  $HO_x$  families are dominated by O and H, respectively. The change in the diurnal behavior of these species with altitude illustrate the transition between the photochemically-controlled region below 82 km and the diffusion-controlled region above 90 km. Since the sodium chemistry above 60 km has very little effect on the background neutral chemistry, the above profiles are used for all the different models of sodium considered below.

The results shown in Figure 2 indicate that the  $[O]/[O_3]$  ratio is  $10^2 - 10^3$  between 80 and 90 km. In the absence of temporary reservoirs,  $[Na]$  and  $[NaO]$  would be controlled by the Chapman scheme. The rates for RR1 and RR2 given in Table 1 would then imply a  $[Na]/[NaO]$  ratio of  $10^1 - 10^2$ , placing the atomic sodium peak well below 80 km. Thus, the observed position of the Na peak and the constraints on RR1 and RR2 as suggested by thermal chemical data strongly suggest the existence of temporary reservoirs for atomic sodium.

Our choice of models for the sodium chemistry focuses on the interaction of the Na-NaO species with the temporary reservoirs,  $NaO_2$  and  $NaOH$ . In the chemical scheme illustrated in Figure 1, the interaction between Na and  $NaO_2$  is controlled by the rapid formation of  $NaO_2$ , (reaction RR3), and recycling of  $NaO_2$  to Na-NaO through RR6. Similarly, coupling to  $NaOH$  is controlled by RR7 and the photolysis reaction RR4. Since experimental data exists on both RR3 (Silver et al., 1984b) and RR4 (Rowland and Makide, 1982), our study will concentrate on reactions RR6 and RR7.

Four models were considered, representing different strengths of coupling between the Na-NaO species and the  $NaO_2$  and  $NaOH$  temporary reservoirs. The adopted parameters for these models are listed in Table 3. Model A represents the conditions for weakest coupling to temporary reservoirs consistent with measured kinetic rates. The value adopted for reaction RR6 is small, but sufficient to recycle enough  $NaO_2$  back to Na-NaO so that Na does not disappear completely (Sze et al., 1982) due to the fast rates measured for reaction RR3. Production of  $NaOH$  by RR7 is assumed to be zero. The coupling between NaO-Na and  $Na'$  is weak, since production of  $NaOH$  occurs only via reactions RR10 and RR11 through  $NaO_2$  as an intermediate. Model C represents conditions of maximum coupling to both temporary reservoirs with rates for reactions RR6 and RR7 near the kinetic limit. Models B and D exhibit combinations of strong and weak coupling to the different temporary reservoirs.

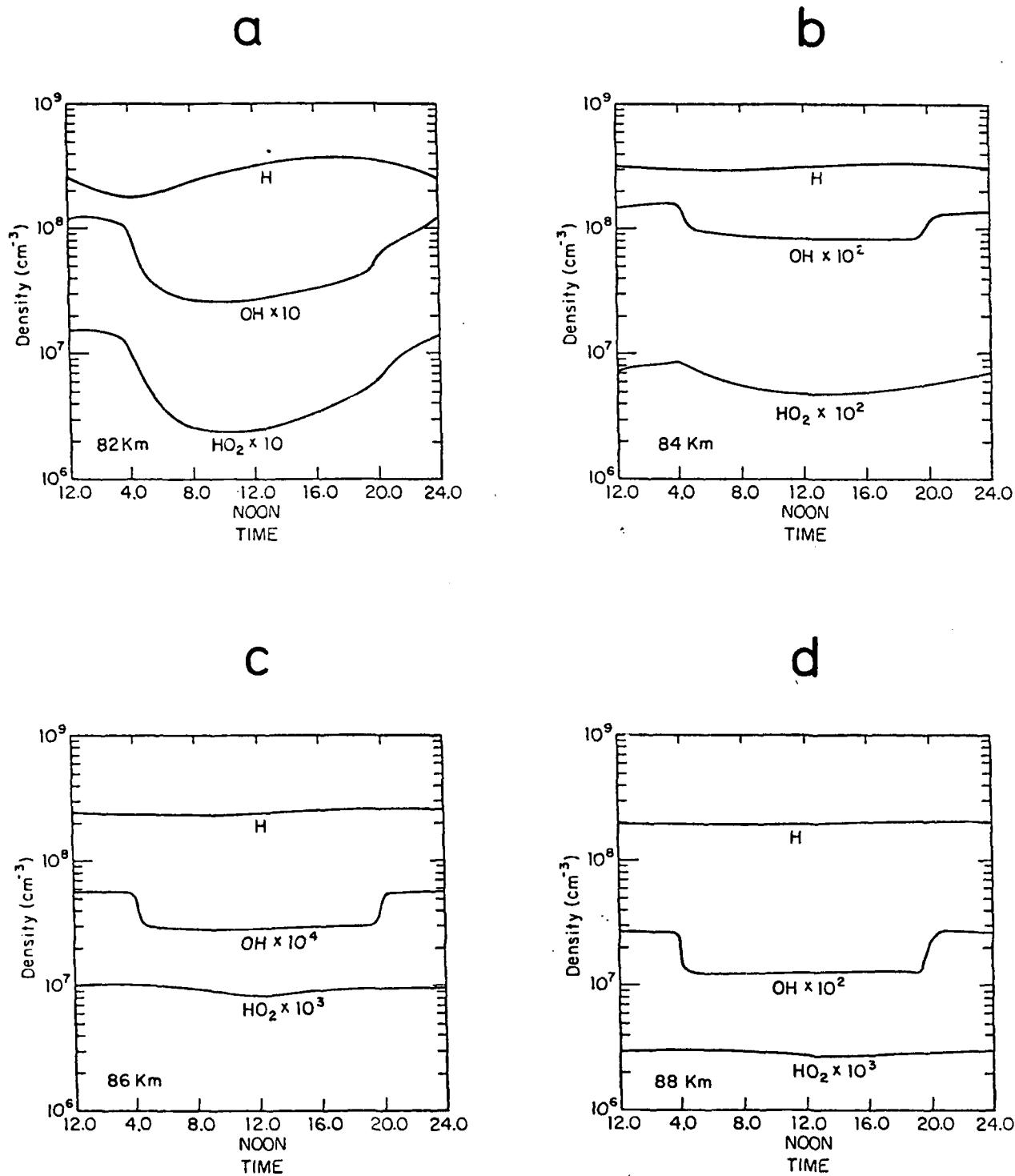


Figure 3. Diurnal variation of odd-hydrogen species H, OH, and HOX calculated at (a) 82 km, (b) 84 km, (c) 86 km, and (d) 88 km.

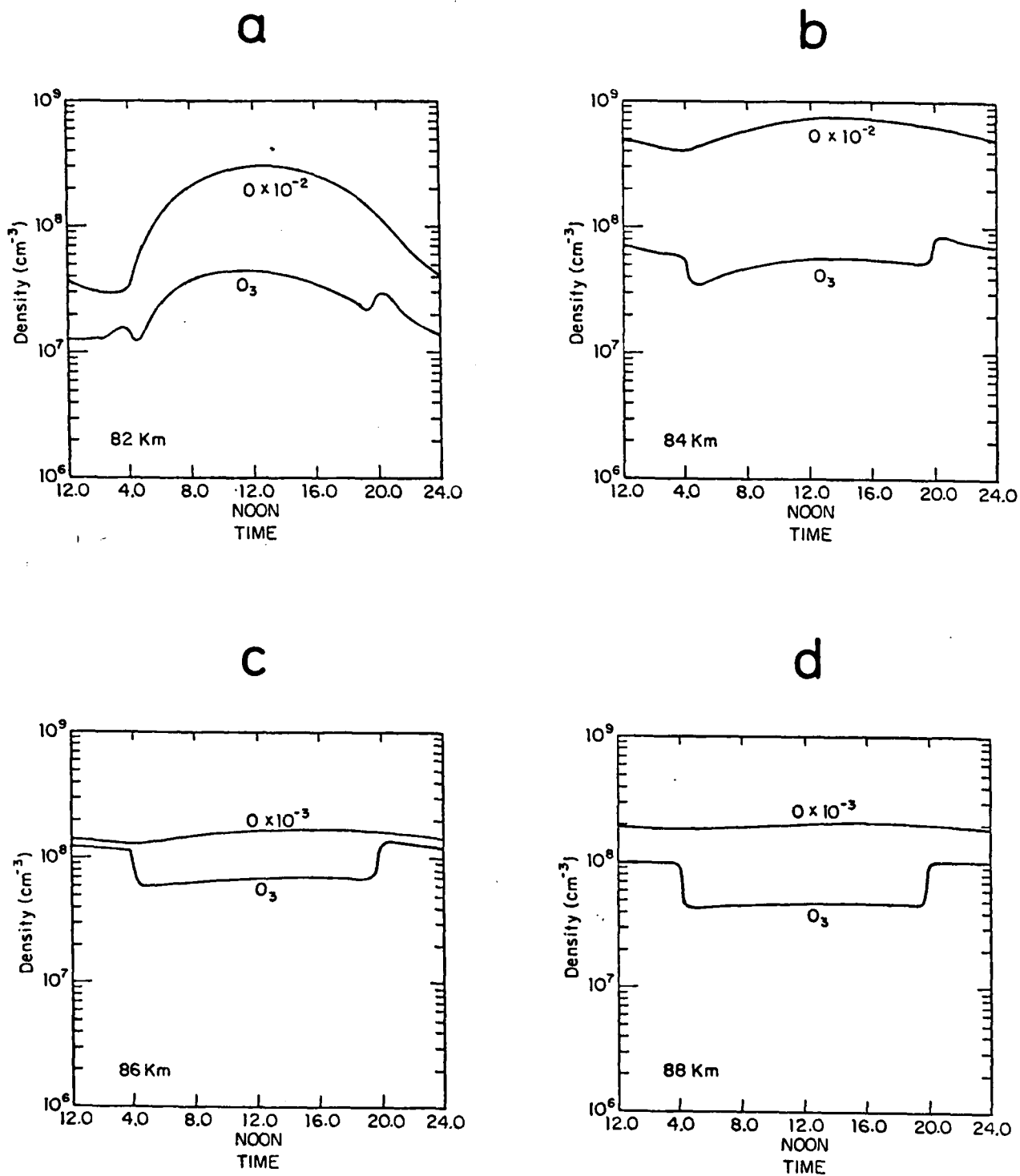


Figure 2. Diurnal variation of odd-oxygen species  $O$  and  $O_3$ , calculated by our model at (a) 82 km, (b) 84 km, (c) 86 km, and (d) 88 km. Input parameters and assumptions of our model are discussed in the text.



## SODIUM CHEMISTRY

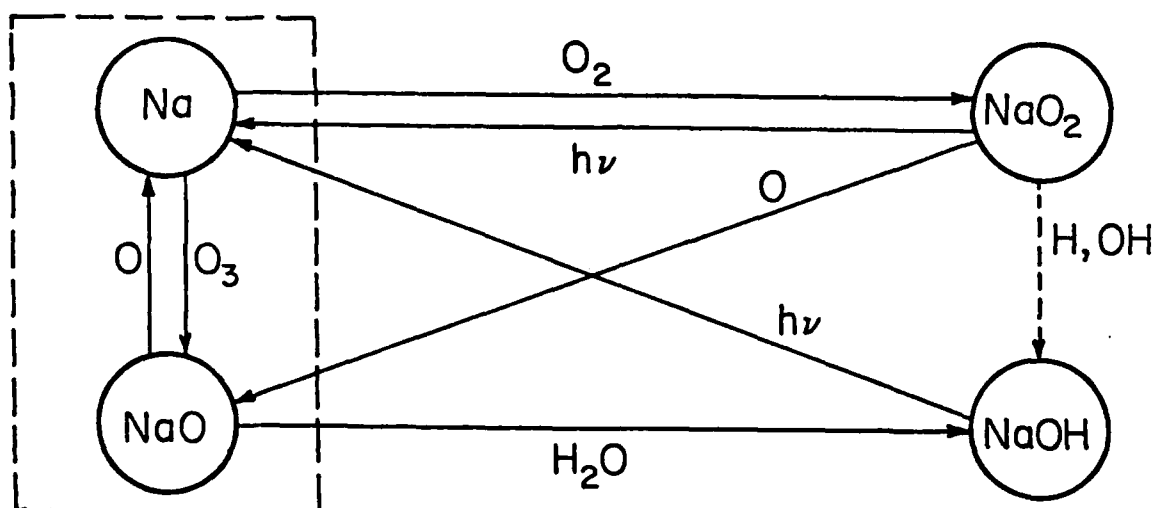


Figure 1. Chemical reactions controlling the behavior of sodium species in the mesosphere. The dotted box in the left-hand side represents the scheme proposed by Chapman (1939). Coupling to the temporary reservoirs NaO<sub>2</sub> and NaOH occurs primarily through the reactions denoted by solid arrows. The dotted arrows represent direct production of NaOH from NaO<sub>2</sub> (Liu and Reid, 1979). This mechanism is the primary source of NaOH if the reaction rate of NaO with H<sub>2</sub>O is negligible.

- Simonich, D. M., B. R. Clemesha, and V. W. J. H. Kirchoff (1979) The mesospheric sodium layer at 23°S: Nocturnal and seasonal variations. J. Geophys. Res. 84, 1543.
- Solomon, S., P. J. Crutzen, and R. G. Roble (1982) Photochemical coupling between the thermosphere and the lower atmosphere. I. Odd nitrogen from 50 to 120 km. J. Geophys. Res., 87, 7206
- Swider, W. (1970) Ionic reactions for meteoritic elements, Ann. Geophys., 26, 595.
- Swider, W. (1984) Ionic and neutral concentrations of Mg and Fe near 92 km, Planet. Space Sci., 32, 307.
- Sze, N. D., M. K. W. Ko, R. Specht, and M. Livshits (1980) Modeling of chemical processes in the troposphere and stratosphere. AFGL-TR-80-0251, Contract No. F 19628-78-C-0215, ADA092704.
- Sze, N. D., M. K. W. Ko, W. Swider, and E. Murad (1982) Atmospheric sodium chemistry. I. The altitude region 70-100 km. Geophys. Res. Lett., 9, 1187-1190.
- Thomas, L., M. C. Isherwood, and M. R. Bowman (1983) A theoretical study of the height distribution of sodium in the mesosphere. J. Appl. Terr. Phys., 45, 587.
- U. S. Standard Atmosphere, 1976 (1976) NA00-S/T 76-1562, Washington, D.C.

- JPL (1982) Chemical kinetics and photochemical data for use in stratospheric modeling. Evaluation #5. JPL Publication 82-57.
- Kirchoff, V. W. J. H. (1983) Atmospheric sodium chemistry and diurnal variations: An update, Geophys. Res. Lett., 10, 721.
- Kirchoff, V. W. J. H., B. R. Clemesha, and D. M. Simonich (1981) Average nocturnal and seasonal variations of sodium nightglow at 23°S, 46°W, Planet. Space Sci., 29, 765.
- Kirchoff, V. W. J. H., and B. R. Clemesha (1983) The atmospheric neutral sodium layer, 2. Diurnal variations, J. Geophys. Res., 88, 442.
- Kolb, C. E., and J. B. Elgin (1976) Gas phase chemical kinetics of the Na in the upper atmosphere, Nature, 263, 488.
- Kvifte, G. (1973) Alkali chemistry problems of the upper atmosphere. In Physics and Chemistry of the Upper Atmosphere, B. M. McCormac (ed.), p. 158, Reidel, Dordrecht, Holland.
- Liu, S. C., and G. C. Reid (1979) Sodium and other minor constituents of meteoric origin in the atmosphere. Geophys. Res. Lett., 6, 283.
- Megie, G., and J. E. Blamont (1977) Laser sounding of atmospheric sodium: Interpretation in terms of global atmospheric parameters, Planet. Space Sci., 25, 1093.
- Megie, G., F. Bos, J. E. Blamont, and M. L. Chanin (1978) Simultaneous nighttime lidar measurements of atmospheric sodium and potassium, Planet. Space Sci., 26, 27.
- Murad, E., and W. Swider (1979) Chemistry of meteor metals in the stratosphere. Geophys. Res. Lett., 6, 929.
- Murad, E., W. Swider, and S. W. Bensen (1981) Possible role for metals in stratospheric chlorine chemistry. Nature, 289, 273.
- Richter, E. S., and C. F. Sechrist, Jr. (1979) A cluster ion chemistry for the mesospheric sodium layer. J. Atmos. Terr. Phys., 41, 579.
- Rowland, F. S., and Y. Makide (1982) Upper stratospheric photolysis of NaOH. Geophys. Res. Lett., 9, 473-475.
- Rowland, F. S., and P. J. Rogers (1982) Upper stratospheric photolysis of NaCl and KCl, Proc. Nat. Acad. Sci. USA, 79, 2737.
- Silver, J. A., A. C. Stanton, M. S. Zahniser, and C. E. Kolb (1984a) The gas phase reaction rate of sodium hydroxide with hydrochloric acid, J. Phys. Chem. (in press).
- Silver, J. A., M. S. Zahniser, A. C. Stanton, and C. E. Kolb (1984b) Temperature-dependent termolecular reaction rate constants for potassium and sodium peroxide formation. Presented at the 20th International Symposium on Combustion, the Combustion Institute, Pittsburgh, PA.

### References

- Allen, M., J. I. Lunine, and Y. L. Yung (1984) The vertical distribution of ozone in the mesosphere and lower thermosphere, J. Geophys. Res., 89, 4841.
- Arnold, F., H. Böhrringer, and G. Henschen (1978) Composition measurements of stratospheric positive ions, Geophys. Res. Lett., 5, 653.
- Arnold, F., G. Henschen, and E. E. Ferguson (1981) Mass spectrometric measurements of fractional ion abundances in the stratosphere-positive ions, Planet. Space Sci., 29, 185.
- Bates, D. R., and P. C. Ojha (1980) Excitation of the Na D-doublet of the night-glow, Nature, 286, 790.
- Chapman, S. (1939) Notes on atmospheric sodium, Ap. J., 90, 309.
- Clemesha, B. R., V. W. J. H. Kirchoff, and D. M. Simonich (1978) Simultaneous observations of the Na 5893Å nightglow and the distribution of sodium atoms in the mesosphere, J. Geophys. Res., 239, 509.
- Clemesha, B. R., D. M. Simonich, P. O. Batista, and V. W. J. H. Kirchoff (1982) The diurnal variation of atmospheric sodium, J. Geophys. Res., 87, 181.
- Ferguson, E. E. (1978) Sodium hydroxide ions in the stratosphere, Geophys. Res. Lett., 5, 1035.
- Fukuyama, K. (1977) Airglow variations and dynamics in the lower thermosphere and upper mesosphere, II, Seasonal and long-term variations, J. Atmos. Terr. Phys., 39, 1.
- Gadsden, M. (1968) Sodium in the upper atmosphere: meteoritic origin, J. Atmos. Terr. Phys., 30, 151.
- Gibson, A. J., and M. C. W. Sandford (1971) The seasonal variation of the night-time sodium layer, J. Atmos. Terr. Phys., 33, 1675.
- Gibson, A. J., and M. C. W. Sandford (1972) Daytime laser radar measurements of the atmospheric sodium layer, Nature, 239, 509.
- Granier, C., and G. Megie (1982) Daytime lidar measurements of the mesospheric sodium layer. Planet. Space Sci., 30, 169.
- Hunten, D. M. (1975) Vertical transports in atmospheres. In Atmospheres of Earth and Planets. B. M. McCormac (ed.), Dordrecht, Holland, pp. 59-72.
- Hunten, D. M., R. P. Turco, and O. B. Toon (1980) Smoke and dust particles of meteoritic origin in the mesosphere and stratosphere, J. Atmos. Sci., 37, 1342.
- Husain, D., and J. M. C. Plane (1982) Kinetic investigation of the reaction between  $\text{Na} + \text{O}_2 + \text{M}$  by time resolved atomic resonance absorption spectroscopy, J. Chem. Soc., Faraday Trans., 2, 78, 163.

Table 4: Calculated Sodium Parameters for the Different Models

	Model A	Model B	Model C	Model D	Measured Value
Peak Altitude	90 km	90 km	86 km	82 km	90-92 km
Peak Density	$4.3 \times 10^3 \text{ cm}^{-3}$	$4.3 \times 10^3 \text{ cm}^{-3}$	$6.3 \times 10^3 \text{ cm}^{-3}$	$9.1 \times 10^3 \text{ cm}^{-3}$	$3-5 \times 10^3 \text{ cm}^{-3}$
Total Abundance <sup>a</sup>	$4.75 \times 10^9 \text{ cm}^{-2}$	$4.47 \times 10^9 \text{ cm}^{-2}$	$6.34 \times 10^9 \text{ cm}^{-2}$	$1.26 \times 10^{10} \text{ cm}^{-2}$	$2-8 \times 10^9 \text{ cm}^{-2}$
Diurnal Variation, <sup>b</sup> Total Abundance	5%	14%	31%	46%	<15%
$[\text{Na}]_{\text{Dusk}}/[\text{Na}]_{\text{Dawn}}$	$\frac{6.0 (82 \text{ km})}{1.8 (84 \text{ km})}$	$\frac{8.0 (82 \text{ km})}{2.4 (84 \text{ km})}$	$\frac{25.5 (82 \text{ km})}{3.8 (84 \text{ km})}$	$\frac{1.7 (82 \text{ km})}{1.02 (84 \text{ km})}$	$\frac{10 (81 \text{ km})}{2 (83 \text{ km})}$
D-Line Emission Rate (night)	46 R	39 R	47 R	84 R	50 R

<sup>a</sup>Averaged over one day.

<sup>b</sup>Percent deviation from the median abundance.

Table 2: Experimental Data on Sodium

		<u>References</u>
<u>Sodium Layer</u>		
Peak Altitude	90 - 92 km	Megie and Blamont, 1977;
Peak Density	$3-5 \times 10^3 \text{ cm}^{-3}$	Simonich et al., 1979
Total Abundance	$4 \times 10^9 \text{ cm}^{-2}$ ( $2-8 \times 10^9 \text{ cm}^{-2}$ )	Gibson and Sandford, 1972; Clemesha et al., 1982
<u>Diurnal Variation</u>		
Total Abundance <sup>a</sup>	< 15%	Gibson and Sandford, 1971; Clemesha et al., 1982
[Na] <sub>Dusk</sub> /[Na] <sub>Dawn</sub>	2 (83 km) 10 (81 km)	Simonich et al., 1979; Clemesha et al., 1982
<u>D-line Emission Rate</u>	~ 50 R (30-100 R)	Fukuyama, 1977; Kirchoff et al., 1981

<sup>a</sup>Percent deviation from median abundance

Table 3: Adopted Models

	<u>k (NaO<sub>2</sub> + O)</u> (cm <sup>3</sup> s <sup>-1</sup> )	<u>k (NaO + H<sub>2</sub>O)</u> (cm <sup>3</sup> s <sup>-1</sup> )
Model A	10 <sup>-13</sup>	0.0
Model B	10 <sup>-13</sup>	10 <sup>-10</sup>
Model C	10 <sup>-10</sup>	10 <sup>-10</sup>
Model D	10 <sup>-10</sup>	0.0

Table 1: Reaction Scheme and Rate Constants

Reaction		Rate Coefficient <sup>a</sup>
1. Na + O <sub>3</sub>	→ NaO + O <sub>2</sub>	3(-10) [b]
2. NaO + O	→ Na (2P, 2S) + O <sub>2</sub>	4(-11) [c]
3. Na + O <sub>2</sub> + N <sub>2</sub>	→ NaO <sub>2</sub> + N <sub>2</sub>	1.9 X 10 <sup>-30</sup> (T/300) <sup>-1.1</sup> [d]
4. NaOH + hv	→ Na + OH	2(-3) [e]
5. NaO <sub>2</sub> + hv	→ Na + O <sub>2</sub>	1(-4) [c]
6. NaO <sub>2</sub> + O	→ NaO + O <sub>2</sub>	1(-10), 1(-13) [c]
7. NaO + H <sub>2</sub> O	→ NaOH + OH	0, 1(-10) [c]
8. NaO + O <sub>3</sub>	→ NaO <sub>2</sub> + O <sub>2</sub>	5(-11) [f]
9. NaO + H	→ Na + OH	1(-14) [g]
10. NaO <sub>2</sub> + OH	→ NaOH + O <sub>2</sub>	1(-11) [f]
11. NaO <sub>2</sub> + H	→ NaOH + O	1(-13) [g]
12. NaOH + H	→ Na + H <sub>2</sub> O	1.4(-12) [f]
13. NaOH + ( <sup>1</sup> D)	→ NaO + OH	1(-10) [g]
14. Na + HO <sub>2</sub>	→ NaOH + O	1(-10) [f]
15. NaO + O <sub>3</sub>	→ Na + 2O <sub>2</sub>	1(-10) [g]
16. NaO + HO <sub>2</sub>	→ NaOH + O <sub>2</sub>	1(-11) [f]

<sup>a</sup>Read 3(-10) as 3 x 10<sup>-10</sup>. Units are cm<sup>3</sup> s<sup>-1</sup>, except cm<sup>6</sup> s<sup>-1</sup> for (3) and s<sup>-1</sup> for (4), (5), and (15). [b], Kolb and Elgin (1976). [c], Sze et al. (1982). [d], Silver et al. (1984). [e], Rowland and Makide (1982). [f], Liu and Reid (1979). [g], Kirchoff and Clemesha (1983).

change with  $O_2^+$ , with an effective J rate of  $\sim 10^{-5} \text{ s}^{-1}$  (Swider, 1970; 1984). Loss of  $Na^+$  occurs primarily through clustering with  $N_2$ ,



followed by dissociative recombination of  $Na^+ \cdot N_2$  (Richter and Sechrist, 1979). The partitioning between Na and  $Na^+$  is determined by the rate of the clustering reaction (7), which has not been measured. If one uses the estimated rate (Richter and Sechrist, 1979) based on analogous reactions involving  $NO^+$ , as much as half of the atomic sodium could be in ionized form at 100 km. This would reduce the amount of atomic Na calculated in the model and introduce diurnal variation of Na at these altitudes bringing the result into much better agreement with the measurements shown in Figure 4. Ionization of Na could thus account for the small Na scale height (2 to 3 km) observed above the peak (Simonich et al., 1979; Granier and Megie, 1982).

In conclusion, the results of our study point out the importance of the  $NaO_2$  temporary reservoir in determining the diurnal variation of atomic sodium. The diurnal variation of atomic oxygen thus plays a dominant role in determining diurnal changes in Na. Present experimental data constrains the recycling of  $NaO_2$  through reaction with O (RR6), limiting the rate to considerably less than  $10^{-10} \text{ cm}^3 \text{ s}^{-1}$ , but at least  $10^{-13} \text{ cm}^3 \text{ s}^{-1}$ . The data, however, does not rule out production of large amounts of NaOH through the reaction of NaO with  $H_2O$  (reaction RR7). Further clarification of this problem requires measurements of unknown reaction rates (in particular, RR4, RR5, RR6, and RR7), continuing high-resolution observations of sodium species in the upper atmosphere, and further modelling incorporating tidal and gravity wave effects on both sodium species and background trace gases.



Figure 2 and that of Na in Figure 6 suggests general agreement between both diurnal changes. In fact, the ratio  $[O]_{\text{Dusk}}/[O]_{\text{Dawn}}$  is 5.3 at 82 km and 1.7 at 84 km, similar to the sodium ratio in Model A. The additional coupling to NaOH is reflected in larger ratios for Models B and C. Since the sodium peak is at 82 km for Model D, NaO<sub>2</sub> is no longer the major sodium species, and the local nocturnal variation is smaller than for the previous models.

Given that diurnal variation of atomic sodium depends crucially on the diurnal variation of atomic oxygen, the observed absence of appreciable diurnal change in the total Na abundance requires that the bulk of the sodium be located in a region where O is constant throughout the day, i.e., about 85 km. Once the total NaX is fixed, the position of the peak is determined to first order by the magnitude of RR3. Lowering the peak by modifying the NaX profile through changes in the Na source or eddy diffusion coefficient could be reflected in a larger diurnal variation of the column density of sodium. Since the time constant for the Na-NaO<sub>2</sub> exchange ranges from seconds to a few minutes below 90 km, any modelling of transport effects (i.e., tides, gravity waves) must include a self-consistent treatment of the atomic oxygen variation.

The photolytic reactions,



could also play an important role in the diurnal variation of sodium if their values were very different from those assumed here. Reaction RR5 could compete with the reaction with O (RR6) if  $J_5 \sim 10^{-2} \text{ s}^{-1}$ . In such a case, the recycling of NaO<sub>2</sub> to Na would occur via reaction RR5, and the constraints derived here for reaction RR6 can be easily translated into similar constraints for reaction RR5. Photolysis of NaO<sub>2</sub> is also important in the stratosphere, where the concentration of atomic oxygen is small.

The value adopted for reaction RR4 by Rowland and Makide (1982) assumes that all the observed EUV absorption of NaOH is due to photolysis. If this is not the case, and  $J_4$  is smaller, our models would produce more NaOH, its day-to-night change would be smaller and the effects of coupling of Na-NaO to the NaOH reservoir would be consequently reduced.

Ionization of atomic sodium can also affect our results in the region above the peak. Atomic sodium is ionized both by photons and by charge ex-

## 5. DISCUSSION AND CONCLUSIONS

Results of Models A, B, C, and D are summarized in Table 4. The experimental results from Table 2 are included for comparison. Also shown in Table 4 is the midnight D-line emission rate. Results on the D-line emission rate are reasonable for all models, and thus are inconclusive for our purposes. As noted previously, Models C and D agree poorly with observations of the peak height, peak density, the column density, and its diurnal variation. We can therefore rule out Models C and D as unrealistic descriptions of sodium chemistry in the upper atmosphere. The rate for RR6 ( $\text{NaO}_2 + \text{O} \rightarrow \text{NaO} + \text{O}_2$ ) must therefore be significantly lower than  $10^{-10} \text{ cm}^3 \text{ s}^{-1}$ , closer to  $10^{-13} \text{ cm}^3 \text{ s}^{-1}$ .

It is harder to draw any definite conclusions to differentiate between Models A and B. The best basis for differentiation is the diurnal variation of local densities and total column densities of Na. Local density variations for both models are consistent with observations, given the altitude resolution of lidar measurements. Variations in the total column density for Models A and B are more sharply differentiated, and the question thus lies on the interpretation of the experimental data.

Early lidar measurements of the sodium layer yielded day-to-night ratios of at most 10% (Gibson and Sandford, 1972) or changes during the night of about 4% (Simonich et al., 1979). More recent observations of Clemesha et al. (1982) which were carried out on a continuous basis yielded diurnal variations with an amplitude of  $\sim 15\%$  from the mean (30% peak-to-peak). The observations, however, exhibited a strong semidiurnal component, and the above authors suggested that the diurnal variation is due entirely to tidal effects. Thus, definite conclusions could be made only after incorporation of tidal effects into existing photochemical models, coupled with higher resolution measurements of the diurnal variation of Na. We thus conclude that a rate of  $10^{-10} \text{ cm}^3 \text{ s}^{-1}$  for RR7 ( $\text{NaO} + \text{H}_2\text{O} \rightarrow \text{NaOH} + \text{OH}$ ) is still consistent with present experimental data.

Another consequence of the high rate for reaction RR3 is that the diurnal variation of atomic sodium below the peak can be estimated to first order in Models A and B from the photochemical equilibrium relation between Na and  $\text{NaO}_2$  given in equation (5). The diurnal variation of Na then follows that of atomic oxygen if  $\text{NaO}_2$  does not change appreciably, a condition satisfied below the Na peak in Models A and B. Comparison of the diurnal variation of O in

ratio can be estimated from the approximate chemical equilibrium conditions for  $\text{NaO}_2$ :

$$k_3[\text{Na}][\text{O}_2][\text{M}] \sim k_6[\text{NaO}_2][\text{O}]. \quad (5)$$

In both Models A and B, Na is the most abundant species at 90 km. At lower altitudes, with larger values for  $[\text{O}_2]$  and  $[\text{M}]$  and smaller values for  $[\text{O}]$ ,  $\text{NaO}_2$  becomes the most abundant species at 82 km.

In Model A, with production of NaOH from the reactions of  $\text{NaO}_2$  with H and OH alone, the  $[\text{NaOH}]/[\text{NaO}_2]$  ratio is approximately given by

$$(J_4 + k_{12}[\text{H}])[\text{NaOH}] \approx [\text{NaO}_2] (k_{10}[\text{H}] + k_{11}[\text{OH}]). \quad (6)$$

Rapid changes in  $[\text{NaOH}]$  are expected at dawn and dusk due to the onset and disappearance of photolysis. However, the concentration of NaOH in Model A is sufficiently small at 90 km that its variation does not affect the diurnal behavior of Na and  $\text{NaO}_2$  (Figure 7b). There is no calculated diurnal variation for Na and  $\text{NaO}_2$  at 90 km, because O shows no diurnal variation at this altitude (Figure 2). At 82 km, the calculated  $\text{NaO}_2$  shows a higher concentration in the daytime (Figure 7a) because of the interconversion with NaOH which has comparable concentration during the night. The diurnal variation of Na follows closely that of O as suggested by the relation in equation (5).

In Model B, equation (6) has to be modified to include an additional source from the reaction of  $\text{NaO} + \text{H}_2\text{O}$ . As a result, the calculated  $[\text{NaOH}]$  is much higher than in Model A. Because of its larger concentration, NaOH is more effective in influencing the diurnal behavior of Na and  $\text{NaO}_2$ . For instance, a slight diurnal variation is seen in both Na and  $\text{NaO}_2$  at 90 km (Figure 7d). At 82 km, however, the diurnal behavior of Na is still primarily controlled by the behavior of O.

The primary difference between Models A and B lies in the concentration of NaOH which has not been observed. Unfortunately, NaOH exerts only a second-order effect on the diurnal variations of Na making it difficult to differentiate between the two models based on Na observations.

Noon altitude profiles for Na are shown in Figure 4 for the different models. Measurements by Simonich et al. (1979) for midnight, and Granier and Megie (1982) for noon are also shown at altitudes above 85 km. As indicated by the data, the diurnal variation of Na is negligible between 85 and 95 km. Agreement between these measurements and models C and D is poor. Better agreement is obtained with Models A and B, especially in the region of the peak. The discrepancy between observation and the calculated results above 95 km is probably due to the effect of ion chemistry. We will discuss this in more detail in the next section.

The diurnal variation of the total Na abundance is presented in Figure 5, again for all four models. The absolute magnitude of the abundance is in good agreement with observed values for Models A, B, and C, while Model D yields column densities higher than those observed for average conditions. The diurnal variation of the total abundance is consistent with observations for Models A and B (5% and 15%, respectively), but is too large for Models C and D (30% and 45%, respectively). The large diurnal variations calculated for Models C and D follow from the results that much of the sodium is found below 82 km where the diurnal deviations of Na is the largest.

The results presented in Figures 4 and 5 suggest that Models C and D do not reproduce the observed Na altitude profile and diurnal variation of the sodium abundance. Models A and B yield very similar results. Further discrimination between these two models would have to be based on the diurnal behavior of the sodium species at specific altitudes.

Figures 6a and 6b illustrate the diurnal variation of Na at 82, 84, and 86 km, for Models A (Figure 6a) and B (Figure 6b). Although the diurnal variation in Model B is slightly larger than in A, both models yield results in satisfactory agreement with experimental data. We should note that the day-to-night ratio changes dramatically over an altitude range of 2 km in this region. This fact should be kept in mind in comparing theoretical results to lidar observations, since the latter typically have an altitude resolution of 1 - 2 km (Megie and Blamont, 1977; Simonich et al., 1979).

The interaction between the different sodium reservoirs is illustrated in Figures 7a through 7d. The results can readily be explained in terms of the reaction rates assumed for each model. In the region 80-90 km, the  $[Na]/[NaO_2]$

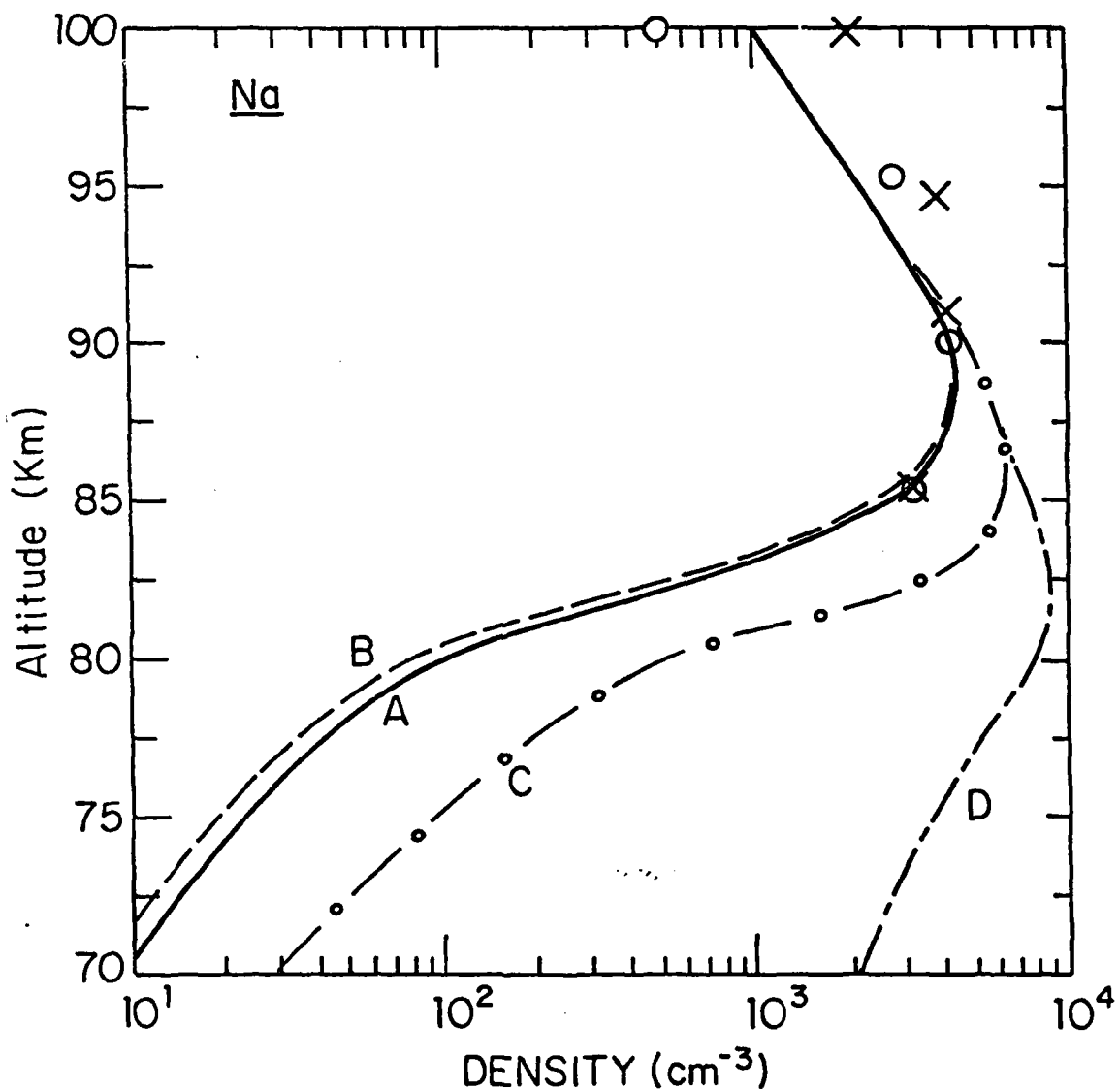


Figure 4. Altitude profiles of atomic sodium at noon calculated for models A, B, C, and D. The measurements of Simonich et al. (1979) at midnight (x) and of Granier and Megie (1982) at noon (o) are also included for comparison.

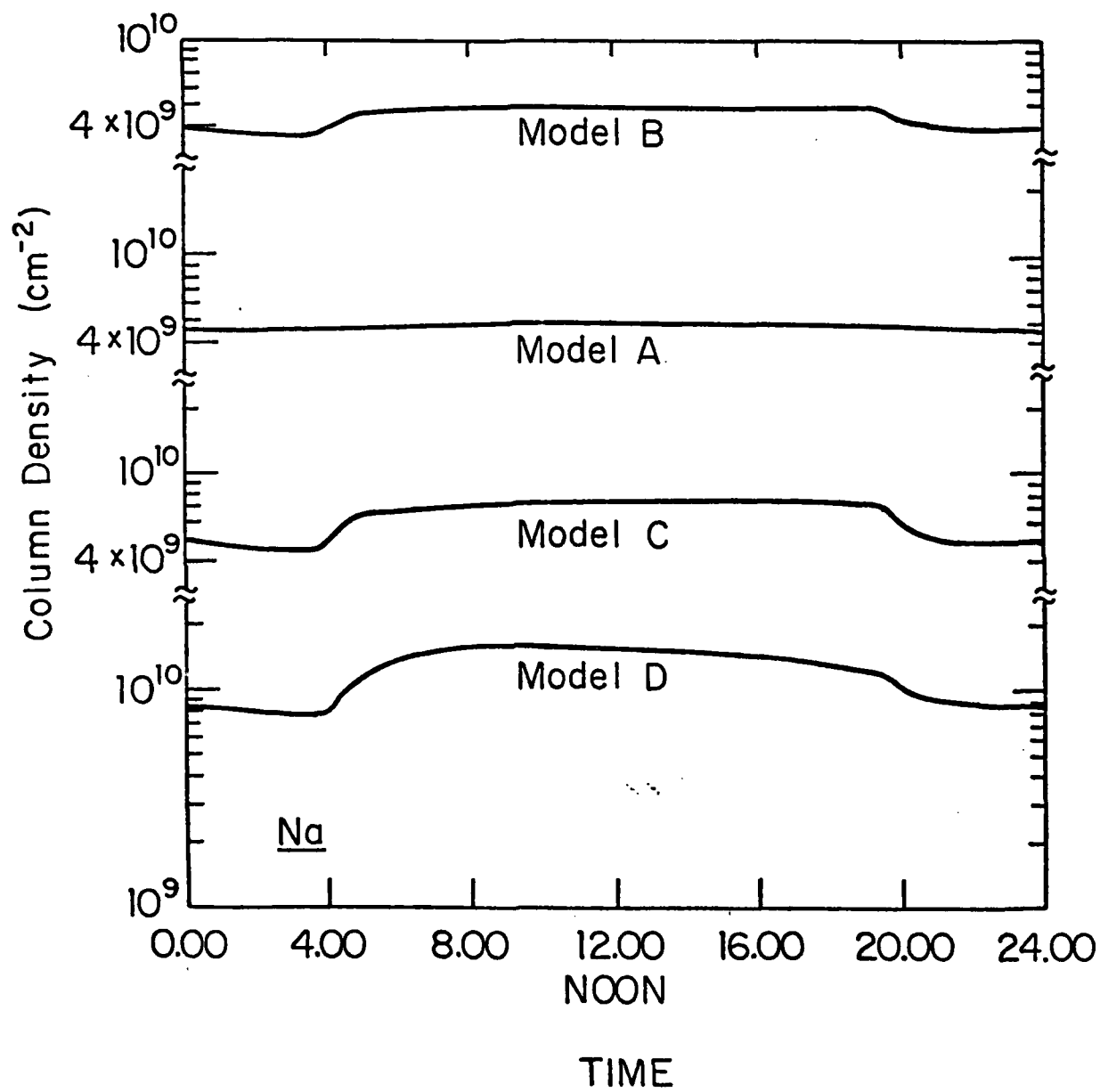
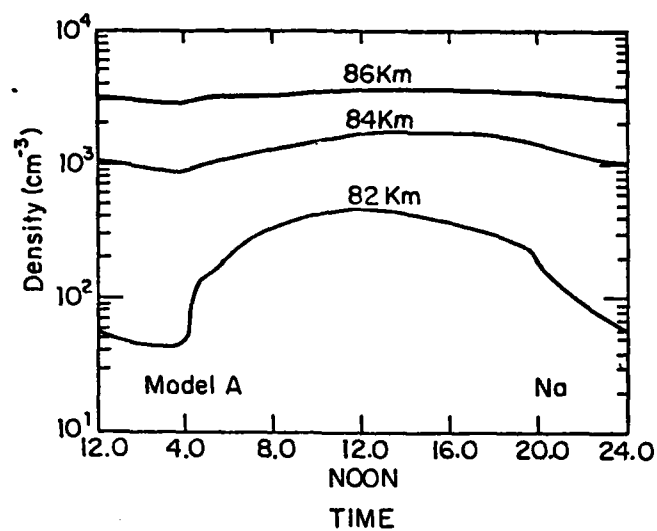


Figure 5. Diurnal variation of the total column abundance of atomic sodium, calculated for models A, B, C, and D.

a



b

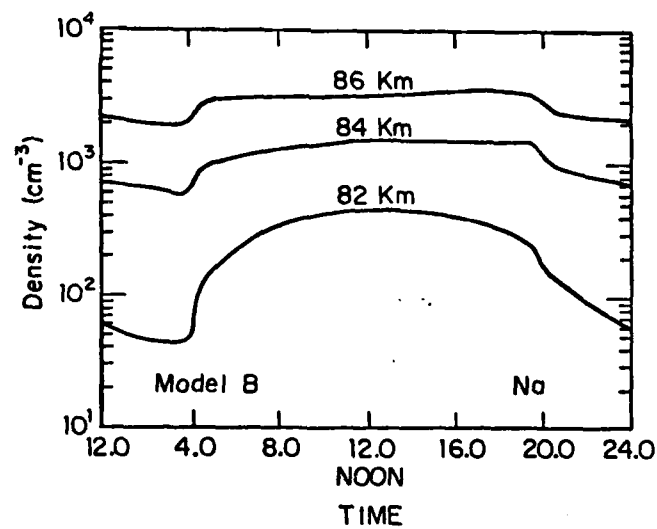


Figure 6. Diurnal variation of local densities of atomic sodium at 82, 84, and 86 km. Results are shown for Model A (6a) and Model B (6b).

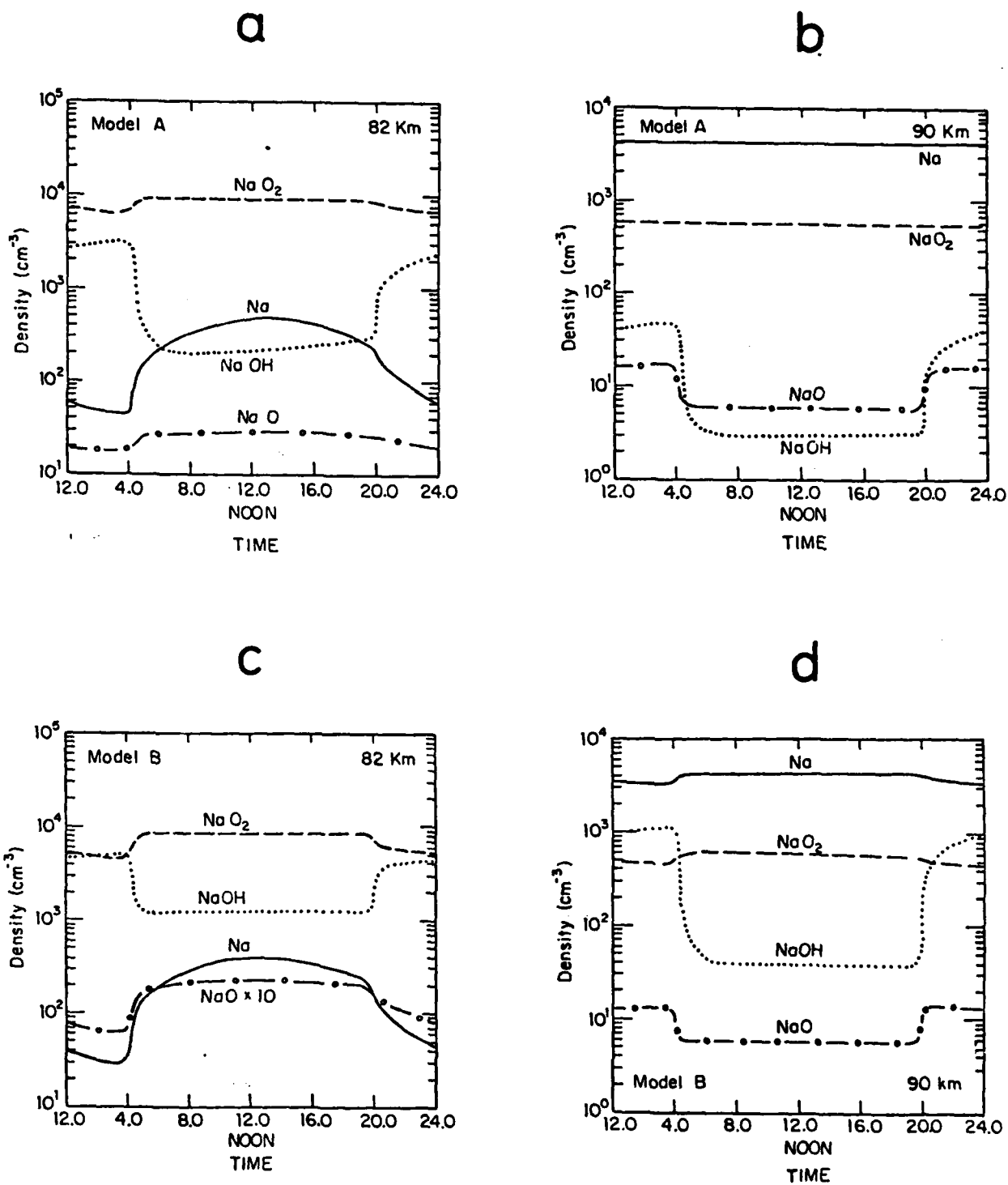


Figure 7. Diurnal variation of the local densities of sodium species at 82 and 90 km, calculated for Model A (7a and 7b) and Model B (7c and 7d).



**END**

**FILMED**

**7-85**

**DTIC**